AIP ADVANCES **6**, 015007 (2016)

Electronic states in spherical GaN nanocrystals embedded in various dielectric matrices: The k·p-calculations

A. A. Konakov,[1,a] D. O. Filatov,[1] D. S. Korolev,[1] A. I. Belov,[1]
A. N. Mikhaylov,[1] D. I. Tetelbaum,[1] and Mahesh Kumar[2]
[1]*Lobachevsky University, Nizhny Novgorod 603950, Russia*
[2]*Department of Electrical Engineering, Indian Institute of Technology Jodhpur, Jodhpur 342011, India*

(Received 26 November 2015; accepted 4 January 2016; published online 11 January 2016)

Using the envelope-function approximation, the single-particle states of electrons and holes in spherical GaN nanocrystals embedded in different amorphous dielectric matrices (SiO_2, Al_2O_3, HfO_2 and Si_3N_4) have been calculated. Ground state energies of electrons and holes in GaN nanocrystals are determined using the isotropic approximation of the $\mathbf{k} \cdot \mathbf{p}$ -Hamiltonian. All the ground state energies are found to increase with lowering the nanocrystal size and are proportional to the R^{-n}, where R is the nanocrystal radius, n =1.5-1.9 for electrons and 1.7-2.0 for holes. The optical gap of GaN nanocrystals changes from 3.8 to 5 eV for the nanocrystal radius ranging from 3 to 1 nm. [http://dx.doi.org/10.1063/1.4939938]

I. INTRODUCTION

Gallium nitride has recently attracted increasing attention due to its importance for the microelectronic and optoelectronic applications.[1,2] It is dictated by such valuable properties of this semiconductor as direct band gap, high carrier mobility, high breakdown field, and high chemical and thermal resistance. In addition, the application of GaN-based alloys enables obtaining the luminescence and optical response in the very wide spectral range, overlapping the ultraviolet, visible and near-infrared region. Unfortunately, the technology of bulk GaN structures is too time-consuming and expensive for mass production. Therefore, currently the main method for obtaining GaN-based structures is their epitaxial growth on sapphire substrates. However, this method does not fully satisfy the trend of modern microelectronics, i.e. the desire to integrate novel technological solutions into the silicon-based technology. The usage of silicon substrates for epitaxial growth of structurally perfect GaN layers encounters several difficulties. First of all, the possible growth of cubic GaN (c-GaN) on Si is complicated by the large difference in lattice parameters of Si and c-GaN (about 20%) and in their thermal expansion coefficients. Moreover, GaN is preferably crystallizes in a hexagonal wurtzite phase (w-GaN) and its structure sufficiently differs from the diamond structure of Si.

There have been more or less successful attempts to overcome these difficulties through the formation of buffer layers.[3,4] However, the techniques used during the fabrication process significantly complicate the technology and lead to a more expensive product. Recently, the application of ion implantation as a method of synthesis of direct band gap semiconductors on silicon have attracted great interest.[5] This method allows creating binary semiconductor inclusions by combined ion implantation of their constituent parts into a variety of matrices, including films on silicon surface. In this way, several attempts to synthesize GaN nanocrystals in silicon and dielectric films on silicon have been made.[6–8]

[a]Corresponding author E-mail: anton.a.konakov@gmail.com

Nanocrystals embedded into wide-band dielectric matrix can have electronic and optical properties of quantum dots. The formation of quantum dots in different dielectric matrices and manipulation of their sizes should offer the possibility to control the luminescence spectrum of such a heterosystem. Effective application of semiconductor nanoinclusions in dielectric matrices in micro- and optoelectronics requires knowledge of their electronic structure. Unfortunately, to the best of our knowledge, there are no data on electronic structure of GaN quantum dots embedded into dielectric films. Moreover, it is at all unclear whether they can acquire properties of quantum dots. This problem is important not only from a fundamental, but also from a practical viewpoint, because the formation of quantum dots in different dielectric matrices and manipulation of their sizes should offer the possibility to control the luminescence spectrum of such a heterosystem.

In this paper, we report on the results of theoretical calculations of electronic spectra of GaN nanocrystals embedded in several dielectric matrices (SiO_2, Al_2O_3, HfO_2 and Si_3N_4). The SiO_2 matrix is the "native" matrix for silicon and is most widely used in silicon-based technology. Al_2O_3 and HfO_2 are the *high-k* dielectrics which are now employed in order to solve the problem of thin insulator layers in CMOS-technology. The silicon nitride Si_3N_4 is the material bridging the "gap" between Si and GaN due to the presence of both silicon and nitrogen atoms and might become the promising matrix compatible with Si-based micro- and nanoelectronics for the formation of GaN nanocrystals. Thereby, our calculations could answer the question which Si/dielectric/GaN structures would have more promising properties for the application in micro- and optoelectronics.

II. METHOD OF CALCULATION

Electronic states in nanocrystals embedded into different matrices have been intensively calculated during last 20 years. For example, electron and hole spectra of silicon quantum dots in dielectric matrices have been well studied.[9,10] Several approaches are widely used to calculate the electronic structure of nanocrystals, such as density functional calculations,[11] *GW* approximation,[12] empirical pseudopotential method,[13] tight-binding approximation[14] and envelope function approximation (EFA).[15] In the present work, the electron and hole states in GaN crystallites of both cubic and hexagonal phases are calculated using the EFA which is sometimes called the $\mathbf{k}\cdot\mathbf{p}$ -method.

Electronic states are determined from the solution of the single-particle Schrödinger-like equation for the envelope function $\psi(\mathbf{r})$:

$$\left(\hat{H}_{\mathbf{k}\cdot\mathbf{p}}(-i\nabla) + U(\mathbf{r})\right)\psi(\mathbf{r}) = E\psi(\mathbf{r}), \tag{1}$$

where $\hat{H}_{\mathbf{k}\cdot\mathbf{p}}(\mathbf{k})$ is the $\mathbf{k}\cdot\mathbf{p}$ -Hamiltonian near the conduction or valence band extremum, where the quasi-wavevector $\mathbf{k}$ is replaced by the differential operator $-i\nabla$ (the first term in the left side of eq. (1) plays the role of effective kinetic energy for the particle in a nanocrystal), $U(\mathbf{r})$ is the effective potential energy of the particle in a nanocrystal, and E stands for the energy of the single-particle state. If the electron states are under consideration, one can use directly the $\mathbf{k}\cdot\mathbf{p}$ -Hamiltonian for the conduction band of bulk crystal. If the hole states are examined, then the kinetic energy term in the valence band Hamiltonian should be used with inverse sign. Due to fast exponential decay of the envelope function into the bulk of surrounding dielectric, it is possible to neglect the difference between the $\mathbf{k}\cdot\mathbf{p}$ -Hamiltonian inside the quantum dot and outside it.[16] In other words, the kinetic energy term is uniform in the system.

The choice of the EFA method is determined by its several advantages over other computational tools for the calculation of the spectra of nanostructures. First, all methods except $\mathbf{k}\cdot\mathbf{p}$ -calculations require a lot of computational resources and therefore can be applied only to nanocrystals with small radii, not more than 1-1.5 nm as a rule, while crystallites synthesized in dielectric matrices by ion implantation typically have larger sizes[5,17] including the case of GaN nanocrystals.[18,19] Second, to calculate the energy spectra and the optical gap of a nanocrystal, the dangling bonds at its surface should be saturated. This problem is nontrivial in cluster methods, when there is a significant difference between the element composition of the nanocrystal and its environment, like for the case of GaN nanocrystals in the mentioned above Si-compatible dielectric matrices, except, possibly, silicon

nitride. As to the $\mathbf{k} \cdot \mathbf{p}$ -method, the surface passivation is effectively modeled by different types and magnitudes of band discontinuities on the nanocrystal boundary.

Nevertheless, the EFA method has also some limitations. First, it is applicable only to the nanocrystals with radii more than approximately 1 nm, which electronic structure can reflect the band structure of the bulk crystal. Second, the effects connected with abrupt interfaces are not taken into account in this approach. The contribution of these effects is proportional to the inverse band gap of a material[20] and for the wide band-gap materials it should be rather small. Still, the necessity to know continuous relationships of energy characteristics with nanocrystal radii in a wide range of their sizes in order to calculate the different response functions of nanocrystal arrays (absorption coefficient or photoconductivity) requires the application of methods, which allow calculating the size-dependence of energy characteristics. Thereby, the EFA becomes the most pragmatic approach to solve the problem.

We consider a spherical quantum dot with radius R in the range from 1 to 3 nm, where the EFA is valid. The upper value of the nanocrystal radius is limited mainly by the experimentally observed sizes of nanocrystals formed in dielectric films using ion implantation.[21] It is necessary to construct correctly the potential energy term that leads to the modification from the bulk band structure to the electronic states in the nanocrystal, i.e. one need to know the internal structure of the term $U(\mathbf{r})$. The quantum dot is assumed to be embedded into infinite wide-band gap dielectric matrix, so the first contribution to $U(\mathbf{r})$ is defined by the quantum confinement phenomenon. The second contribution to the EFA single-particle equation in embedded nanocrystals is determined by fields of electrostatic images of the particle produced by the discontinuity of dielectric constant at the nanocrystal surface.[22] However, as it was shown in Ref. 23, their contributions into electron and hole energies are by an order of magnitude lower than those governed by the size quantization effect in nanocrystals. That is why we do not take them into account.

In order to provide initial conditions for interband radiative recombination the quantum dot should contain an electron and a hole. Both particles create their own electrostatic fields (including polarization fields) and modify the single-particle spectra of each other. Generally speaking, in this case single-particle states are determined self-consistently as the solution of the system of coupled Schrödinger-like and Poisson equations.[24] Nevertheless, such system can be solved perturbatively if the nanocrystal radius R is less than the hydrogen-like Bohr radius a_B of exciton in bulk semiconductor:

$$R < a_B \tag{2}$$

In w-GaN according to Ref. 25 $a_B = 3.29$ nm. In c-GaN Bohr radius of exciton can be estimated as 3.44 nm using static dielectric constant 9.7[26] and electron and hole effective masses listed below in Table III. So, the condition (2) is valid for nanocrystals with radii in the range from 1 to 3 nm. Therefore, in the single-particle equations for electron and hole states we neglect electron-hole interaction.

Finally, in order to minimize the influence of strain fields on the energy spectra of crystallites, they are usually produced in the amorphous dielectric films, where the role of stress is significantly lower.[27] Here, we also suppose the dielectric environment to be amorphous and neglect the contribution of strain fields on the energy spectra of crystallites. So, quantum confinement remains the principal phenomenon that leads to the formation of electronic spectra in the embedded quantum dots, and thus the energy $U(\mathbf{r})$ is determined by only band discontinuities at the crystallite/matrix interface.

We denote the finite potential barriers for electrons and holes at the nanocrystal boundary as ΔE_c and ΔE_v, respectively, and suppose them to be constant everywhere outside the quantum dot. In spherical quantum dot the potential energy reflects its symmetry, and we denote it as $U(r)$. By placing the origin of coordinates at the centre of the crystallite, the carrier potential energy can be written as

$$U(r) = \begin{cases} 0, r < R, \\ \Delta E_i, r \geq R, \end{cases} \tag{3}$$

where "i" means "c" for the conduction band discontinuity (potential energy for electrons) and "v" – for the valence band offset (when calculating the hole spectra). Band discontinuities at the

TABLE I. Calculated values of the conduction and valence band discontinuities (ΔE_c and ΔE_v, respectively) at the w-GaN/dielectric interface at room temperature for different dielectrics.[28] E_g stands for the band gap of corresponding dielectric.

Dielectric	E_g, eV	ΔE_c, eV	ΔE_v, eV
SiO_2	9.0	2.6	3.2
Al_2O_3	8.8	2.2	3.4
HfO_2	6.0	1.1	1.6
Si_3N_4	5.3	1.3	0.8

plane interface between w-GaN (the band gap 3.20 eV)[26] and several dielectrics were calculated in Ref. 28. The values ΔE_c and ΔE_v for the systems under consideration at room temperature are presented in Table I. The calculations[28] show that all heterojunctions for these systems are of the first type. We suppose that, at the spherically symmetric boundary of quantum dot, the band offsets remain the same as in the case of planar heterojunction.

Unlike the w-GaN/insulator interface, there is no systematic information about the band discontinuities at the c-GaN/dielectric boundaries in literature (this is probably because GaN usually crystallizes into hexagonal phase during the epitaxial growth). Strictly speaking, the band offsets at the boundary of the same dielectric with cubic and hexagonal GaN should be different. But, the band gaps in both phases of GaN are very close (according to Ref. 26, the band gap of c-GaN is greater by 0.19 eV: 3.39 eV *versus* 3.20 eV for w-GaN), so one can assume that the band offsets for the interfaces of c-GaN and w-GaN with the same dielectric should be very close. As the first approximation, we suppose that both conduction and valence band offsets at the c-GaN/dielectric interface are 0.1 eV smaller than the corresponding values for the w-GaN/dielectric interface (see Table II).

Let us next discuss the kinetic energy term in the effective Hamiltonian for both cubic and hexagonal phases of GaN.

c-GaN

In c-GaN, the conduction band minimum has s-like Γ_1 symmetry, electronic spectrum near the band edge is isotropic and quadratic, thus the $\mathbf{k} \cdot \mathbf{p}$ -Hamiltonian has the form

$$\hat{H}_{CB}^{(c)}(\mathbf{k}) = \frac{\hbar^2 \mathbf{k}^2}{2m_e} \tag{4}$$

with scalar electron effective mass $m_e \approx 0.193 m_0$,[29] where m_0 is the free electron mass. Electronic states near the valence band maximum in c-GaN are triply degenerate (neglecting spin and the spin-orbit interaction), have the orbital p-like symmetry and are described by the 3×3 matrix Hamiltonian (the Luttinger-Kohn Hamiltonian):[13]

$$\hat{H}_{VB}^{(c)}(\mathbf{k}) = \frac{\hbar^2}{2m_0} \begin{pmatrix} A_L k_x^2 + B_L\left(k_y^2 + k_z^2\right) & C_L k_x k_y & C_L k_x k_z \\ C_L k_x k_y & A_L k_y^2 + B_L\left(k_x^2 + k_z^2\right) & C_L k_y k_z \\ C_L k_x k_z & C_L k_y k_z & A_L k_z^2 + B_L\left(k_x^2 + k_y^2\right) \end{pmatrix}, \tag{5}$$

where A_L, B_L and C_L are the Kohn-Luttinger parameters that fully describe quantum states near the maximum of the valence band. Eigenvalues of this Hamiltonian are significantly anisotropic, in

TABLE II. Adopted values of conduction and valence band discontinuities (ΔE_c and ΔE_v, respectively) at the c-GaN/dielectric interface at room temperature for different dielectrics.

Dielectric	ΔE_c, eV	ΔE_v, eV
SiO_2	2.5	3.1
Al_2O_3	2.1	3.3
HfO_2	1.0	1.5
Si_3N_4	1.2	0.7

contrast to the dispersion law near the bottom of the conduction band. The valence band parameters are $A_L \approx 5.05$, $B_L \approx 1.23$, $C_L \approx 5.86$,[29] where the "plus" sign is taken in order to calculate the hole energies.

The spin-orbit interaction leads to a small splitting of the valence band near its maximum, which takes place both in cubic and hexagonal crystals. According to Varguftman *et al.*,[30] the spin-orbit splitting of the valence band is 17 meV for w-GaN. For c-GaN, spin-orbit splitting of the valence band was calculated by Cardona and Christensen[31] using the method of linearized augmented plane waves in the local density approximation for the exchange-correlation functional. The resulting value was 18.5 meV. The spin-orbit splitting in both phases is significantly lower than the typical energies of size quantization in nanocrystals,[9,10] so we will neglect it in our calculations.

w-GaN

The w-GaN phase has lower symmetry than its cubic counterpart (the direction along the axis of symmetry of the 6-th order distinguished from the directions in the plane perpendicular to it, this axis is denoted as the z axis). As shown by Rinke *et al.*,[29] the electronic states at the centre of the Brillouin zone in the wurtzite structure can be formally derived from the electronic states in the cubic phase by implementation of an effective compression along the [111] direction. This leads to the anisotropic conduction band that is characterized by longitudinal m_l and transverse m_t effective masses.[29] In order to calculate the conduction band states in w-GaN nanocrystals, we use the $\mathbf{k} \cdot \mathbf{p}$ -Hamiltonian in the effective mass approximation:

$$\hat{H}_{CB}^{(w)}(\mathbf{k}) = \frac{\hbar^2\left(k_x^2 + k_y^2\right)}{2m_l} + \frac{\hbar^2 k_z^2}{2m_t}. \tag{6}$$

In turn, in the valence band, the threefold degeneracy is partially lifted by the action of the crystal field: it splits into doubly degenerate and non-degenerate bands. The splitting of the valence band induced by the lowering of the symmetry from cubic to hexagonal is approximately 34 meV.[29] This value is significantly lower than the typical energies of size quantization in nanocrystals,[9,10] and we will neglect it in the same manner as we do not take into account the spin-orbit splitting. Besides due to symmetry lowering the number of parameters, which are necessary to write the effective Hamiltonian, increases from three in c-GaN to seven in w-GaN,[29] so the valence band $\mathbf{k} \cdot \mathbf{p}$ -Hamiltonian has the form

$$\hat{H}_{VB}^{(w)}(\mathbf{k}) = \frac{\hbar^2}{2m_0}\begin{pmatrix} L_2k_x^2 + M_2k_y^2 + M_1k_z^2 & N_2k_xk_y & N_1k_xk_z \\ N_2k_xk_y & M_2k_x^2 + L_2k_y^2 + M_1k_z^2 & N_1k_yk_z \\ N_1k_xk_z & N_1k_yk_z & M_3k_x^2 + M_3k_y^2 + L_1k_z^2 \end{pmatrix}. \tag{7}$$

The values of L_1, L_2, M_1, M_2, M_3, N_1, N_2 are reported in Ref. 29. So, the electronic structure of w-GaN quantum dots depends mostly on the symmetry and degeneracy of the bands, not on their inner splitting. As a result, the Hamiltonian (7) is a good approximation for the kinetic energy term near the top of the valence band.

The Rayleigh-Schrödinger perturbation theory was used to solve Eq. (1) for all presented cases, similarly to that was first shown by Burdov[32] for Si nanocrystals. We divide the effective Hamiltonian into two terms: the spherically symmetric Hamiltonian $\hat{H}_0$ and anisotropic term $\hat{H}_1$. The Hamiltonian $\hat{H}_0$ can be calculated via averaging of the effective Hamiltonian over directions in the Brillouin zone of the corresponding GaN phase and can be written in general form as

$$\hat{H}_0 = -\frac{\hbar^2}{2m_a}\hat{L}_0\Delta + U(r), \tag{8}$$

where $\hat{L}_0$ is the unit matrix of the same dimensionality as initial effective Hamiltonian (scalar for the conduction band and 3×3 matrix for the valence band), m_a is an effective mass averaged over directions in the Brillouin zone. The averaged effective masses for all considered cases are presented in Table III.

TABLE III. Effective masses of electrons and holes averaged over directions in the inverse space of the corresponding GaN phase.

Phase of GaN	Band	Averaged effective mass
c-GaN	Conduction band	$0.193m_0$
	Valence band	$0.66m_0$
w-GaN	Conduction band	$0.2m_0$
	Valence band	$0.54m_0$

In order to calculate the envelope functions corresponding to the unperturbed Hamiltonian $\hat{H}_0$ one need to set boundary conditions at the nanocrystal surface for Schrödinger-like equation with the Hamiltonian (8). First, we suppose envelope functions to be continuous at the quantum dot boundary. Second, as was mentioned above we neglect the difference of kinetic energy term inside and outside quantum dot. Therefore, there are no effective mass discontinuity at the quantum dot border, and the second boundary condition is continuity of the radial derivative of the envelope function at the interface. Note also, that the effective mass discontinuity is very important for contacts between semiconductors with low band discontinuities,[33] but at the interfaces under consideration (contacts between wide-band materials) band discontinuities are large enough to neglect this effect in the model.

Thus, the Hamiltonian $\hat{H}_0$ describes the quantum states in spherically symmetric finite barrier quantum well, and we find its eigensystem exactly. The eigenfunctions of the full Hamiltonian was calculated as a linear combination of the s- and p-eigenfunctions of the Hamiltonian $\hat{H}_0$, and the Hamiltonian $\hat{H}_1$, that is the difference between the full Hamiltonian and unperturbed one was treated as a perturbation.

III. RESULTS AND DISCUSSION

Electronic structure of GaN nanocrystals of both cubic and hexagonal phases embedded in different dielectric matrices (SiO_2, Al_2O_3, HfO_2 and Si_3N_4) was calculated using the EFA. The calculations were performed for nanocrystals with radii in the range from 1 to 3 nm. Let us first discuss the eigenvalues for the unperturbed Hamiltonian $\hat{H}_0$. In the spherical potential well of a finite depth, the discrete energy levels may not exist,[34] and it is necessary to determine the minimal radius of the quantum dot, for which at least one discrete energy level ($1s$ in case of spherically symmetric system) exists. We denote this characteristic as *the 1s critical radius* R_{1s} of the nanocrystal. Such characteristic is determined by the band discontinuity at the interface and by the averaged effective mass of carriers:

$$R_{1s}^{(i)} = \frac{\pi\hbar}{2\sqrt{2m_a\Delta E_i}}, \tag{9}$$

where index "i" stands again for "c" or "v". As one can see from (7), the lower effective mass results in the larger critical radius. Therefore, for our purposes, it is enough to calculate the critical radius in the case of the lowest averaged effective mass, i.e. for electrons in the nanocrystal of c-GaN ($0.193m_0$ according to Table III). The similar characteristic can be introduced for each energy level in the spherical quantum well. The critical radius for the corresponding level defines the minimal nanocrystal size, where such level exists. For the $1p$ level, the critical radius is defined as

$$R_{1p}^{(i)} = \frac{\pi\hbar}{\sqrt{2m_a\Delta E_i}}, \tag{10}$$

and is 2 times greater than the corresponding $1s$ critical radius.

Note also that presented above critical radii are calculated using the simplest model of the finite square well. In the more realistic case there are some contributions to the attractive potential of the well such as electron-hole interaction that provide additional confinement of the particle in the quantum dot. In that case the critical radii for all localized states become lower and eq. (9) and (10) are just the upper estimates for the critical radii.

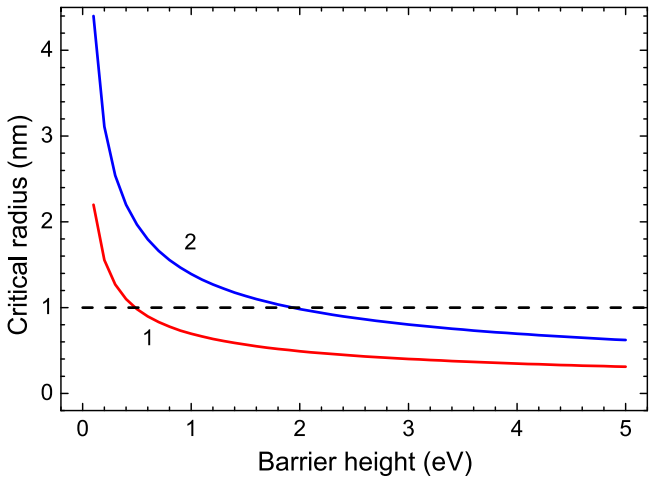

FIG. 1. The dependence of the electron critical radius of c-GaN quantum dot as a function of the band discontinuity (barrier height) at the boundary. The line denoted as "1" corresponds to the $1s$ critical radius, while the line "2" is for the $1p$ critical radius. The horizontal dashed line marks the minimum radius of the nanocrystals that is under consideration in the EFA.

The dependence of the first two electron critical radii of the spherically symmetric c-GaN quantum dot on the nanocrystal size is shown in Fig. 1. The minimal nanocrystal radius is also shown that is under consideration in the frame of EFA. It is seen that for the conduction band discontinuity, which is more than about 0.5 eV, the $1s$ critical radius is less than 1 nm, and thus one can calculate electronic states using the EFA. The $1s$ critical radius for other cases will be smaller because of the larger effective mass. It is shown in Tables II and III, that the lowest barrier height at the nanocrystal boundary is 0.7 eV, so in all the systems under consideration at least one energy level exists in both the conduction and valence bands. Note also that the absolute value of $1p$ critical radius differs significantly from the corresponding value for the $1s$ states. It is lower than 1 nm only for the barrier height greater than 2 eV. Thus, not all quantum dots have the $1p$ energy level. The most important levels for optoelectronic applications are the ground state levels in both the conduction and valence bands of a crystallite, because they determine the energy of the radiative interband transition in a quantum dot. The presence of the localized ground states in the system allows us to calculate the energies of these transitions. So, the ground state energies as functions of the nanocrystal radii and band discontinuities are further considered.

Fig. 2 shows the results of calculations of the ground state energies for electrons and holes in the nanocrystals of both GaN phases. Two upper insets correspond to electron and hole energies in the nanocrystals of c-GaN and two lower ones – to those in w-GaN quantum dots. Let us discuss first the electron states in GaN nanocrystals of both phases. In c-GaN, the dispersion relation in the conduction band is isotropic and electron spectra have the same structure like in conventional spherical quantum wells. Isotropic dispersion relation in the conduction band of c-GaN is valid for the band energies lower than about 1 eV.[35] The calculated electron energies in fact do not exceed this value: they decrease from approximately 1.2 to 0.2 eV with rising the crystallite radius from 1 to 3 nm. So, we assume that our results for electron states in c-GaN quantum dots have a good accuracy. The Hamiltonian eigenvalues correlate with the barrier height for electrons at the nanocrystal boundary: at the same crystallite radius, electron energy has the greater value for the larger band discontinuity. However, in nanocrystals with radii more than 2 nm, the electron ground state energies are almost independent on the band discontinuity. In this case, the quantum well for electrons is too deep to approximate barriers as infinitely high.

In the case of w-GaN nanocrystals, the electron ground state energy is almost the same as in the crystallites of cubic phase due to the following facts: first, the difference between the averaged conduction band effective masses in c-GaN and w-GaN is about only 4%, and, second, the conduction band discontinuities at the interfaces of both GaN phases are modeled to have close values. Besides, the $1s$ and $1p$ states do not mix by the perturbation $\hat{H}_1$ due to its quadratic dependence on the

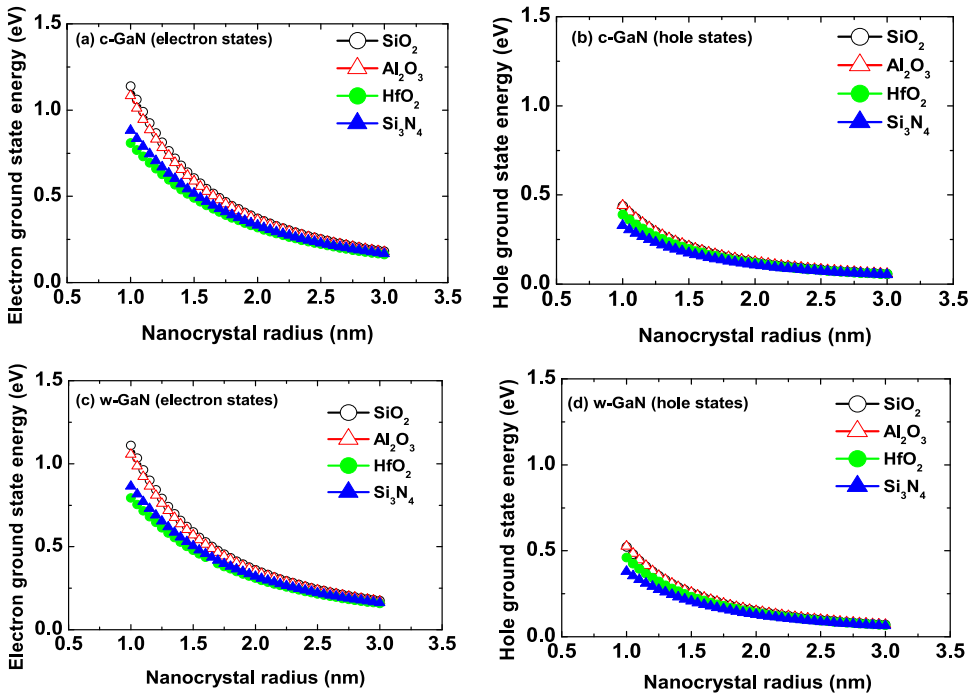

FIG. 2. The dependence of the electron (a, c) and hole (b, d) ground state energies in c-GaN (a, b) and w-GaN (c, d) on the nanocrystal radius.

momentum operator.[32] As well, the upper energy levels of the unperturbed Hamiltonian have too high energies to make significant contribution to the ground state energy in the presence of perturbation. Therefore, the predicted electron energies have a good accuracy for nanocrystals of both GaN phases. All tendencies that characterize the electron ground state energies like the dependence on the band discontinuitites remain the same in w-GaN nanocrystals like in their c-GaN counterparts.

The hole states in GaN crystallites of both lattices are significantly modified in comparison with the conventional spherical quantum wells due to a complex structure of the valence band near its maximum. Moreover, it differs not only qualitatively, but also quantitatively from the electron states because of about 3 times lowering of the averaged effective mass (see Table III). So, it follows from Fig. 2 that the hole energies in w-GaN quantum dots are about 2 times lower than the electron energies at the same radius. For the nanocrystals of c-GaN, this difference is even more expressed. Nonetheless, the perturbation $\hat{H}_1$, which models the anisotropy of the valence band, does not mix the lowest $1s$ state with the closest $1p$ state in both phases, as well as for electrons, as discussed above. Only the upper d-like states will distort the ground state due to anisotropic part of the hole Hamiltonian.[32] By taking this interaction into account, we estimated the accuracy of the ground state calculation in the simple isotropic model of the valence band. So, the isotropic model describes the hole states better in crystallites with smaller radii. For example, in the nanocrystals with radii lower than 2 nm, the computational error reaches the value approximately 1%. In quantum dots with larger sizes, the accuracy of our calculations decreases sufficiently, and the error is about 30% for the nanocrystals with radius of 3 nm. Comparing the hole states in GaN crystallites of both phases, one can notice that the hole ground state energy in the nanocrystals of w-GaN is 15-20% larger than in c-GaN crystallites of the same radii. This fact is trivially explained by the 22% difference in the averaged effective masses of holes in both GaN phases. Another obvious fact is the dependence of the hole states on the valence band discontinuity: increasing the value of ΔE_v produces the increase in the ground hole energy. Nevertheless, as for electrons, the dependence on the band discontinuity is rather weak in the nanocrystals with radii more than 2 nm.

As follows from Fig. 2, the energies of all confined states both in conduction and valence bands depend on the nanocrystal radius that is a direct consequence of the quantum confinement. For the

infinitely deep spherically symmetric quantum dot, the dependence of inverse energy on the nanocrystal radius is always quadratic. However, for the case of *finite* band discontinuities it becomes smoother. One can describe the dependence of the electron and hole energies on the nanocrystal radius in the following form:

$$E_{e(h)} \propto R^{-n}, \tag{11}$$

where the parameter n is itself a function of the quantum dot radius and varies in the range from about 1.5 to about 1.9 for electrons and about 1.7 to about 2.0 for holes, when the radius of nanocrystal increases from 1 to 3 nm. The increase of the parameter n for greater nanocrystal radii is due to lowering the corresponding energy in the nanocrystal: energy decreases and the properties of the finite quantum well become closer to the properties of its infinitely deep counterpart, so the parameter n approaches its limiting value 2.

In order to use the nanocrystals in different optoelectronic devices it is important to know their optical gaps or the energy of the ground electron-hole radiative transition. The nanocrystal optical gap E_{NC} as a function of its radius can be calculated as

$$E_{NC}(R) = E_e(R) + E_h(R) + E_g + E_{e-h}(R), \tag{12}$$

where among the previously defined characteristics, $E_{e-h}(R)$ stands for the correction to optical gap due to the screened Coulomb electron-hole interaction. It contains both direct Coulomb interaction and exchange one. In nanocrystals with R less than the hydrogen-like exciton Bohr radius a_B the direct electron-hole interaction should only insignificantly reduce the optical gap of a crystallite,[23] while exchange coupling leads to the splitting of the degenerate exciton ground state into optically active (bright excitons) and optically passive (dark excitons) states that also depends significantly on the crystalline symmetry.[36] The wavelength of the photon emitted by the nanocrystal is defined by the energy of the low-lying bright exciton, which, according to the reference,[36] should be shifted by only several meV from its unperturbed value. Neglecting this quantity does not affect the interpretation of the luminescence spectra of the nanocrystals' real ensembles due to large number of factors leading to the inhomogeneous broadening of luminescence peak like dispersion of nanocrystals' sizes, their nonuniform distribution in the film and some competitive non-radiative processes in the luminescence kinetics. The quantum confinement remains the principle phenomenon determining the interband recombination in GaN nanocrystals and, thereby, the nanocrystal optical gap can be calculated as

$$E_{NC}(R) = E_e(R) + E_h(R) + E_g. \tag{13}$$

The optical gaps of GaN nanocrystals crystallized in cubic and hexagonal lattices as a function of their radii are plotted in Fig. 3. One can see that, in the crystallites of c-GaN, the optical gap is greater due to the larger value of bulk band gap. In the crystallites of c-GaN, the E_{NC} varies from approximately 5 to 3.7 eV with increase of nanocrystal radius from 1 to 3 nm, while in the quantum dots of w-GaN the optical gap decreases from about 4.8 to 3.5 eV for the same nanocrystal size range. GaN is a direct-band gap semiconductor in both phases, thus, the calculation predicts the possibility of light emission in the UV range of spectrum.

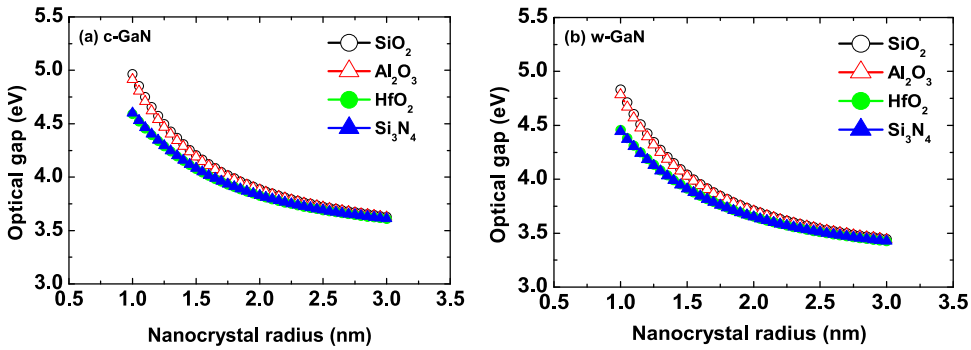

FIG. 3. The dependence of optical gap of c-GaN (a) and w-GaN nanocrystals (b) on the nanocrystal radius.

Comparing the results of the optical gap calculations obtained for GaN quantum dots embedded into different matrices, one can see that the nanocrystals in SiO_2 and Al_2O_3 matrices have greater values of the optical gap than nanocrystals in HfO_2 and Si_3N_4, because of larger magnitudes of band offsets at the GaN/dielectric interface. But, when the nanocrystal radius exceeds 2 nm, such difference becomes negligible: the magnitude of all barriers effectively rises to the limit of their infinitely high counterpart. So, one can expect that the frequency of interband optical transition in GaN nanocrystals will depend on the matrix only for the sufficiently small crystallites.

IV. CONCLUSION

Electronic structure of spherical GaN nanocrystals of both cubic and hexagonal phases embedded in several amorphous dielectric environment (SiO_2, Al_2O_3, HfO_2, Si_3N_4) has been calculated using the envelope function approximation for nanocrystals with radii more than about 1 nm. The calculations show that in all the considered cases there exists at least one electron and one hole level localized in the quantum dot. The energy of radiative transition between these states is in the range from about 3.7 to 5 eV and from approximately 3.5 to 4.8 eV for the nanocrystals of c- and w-GaN, respectively, and depends on the nanocrystal size as a manifestation of the quantum confinement. The optical gap values for small nanocrystals sufficiently exceed the band gap of bulk GaN (3.2 eV in hexagonal GaN and 3.39 eV in cubic phase), so the blue shift of the interband radiation spectra of nanocrystals compared to bulk GaN is expected. Our approach allows to calculate the electron states in the nanocrystals of both GaN phases with sufficiently high accuracy, while the results for holes is not so clear: the computational error can achieve about 30% for the nanocrystals with radii about 3 nm. Such a difference is determined by the anisotropy of the valence band that we do not take into account in our calculations. Nevertheless, the ratios between the electron and hole energies for different matrices as well as between optical gaps in the crystallites of both phases remain the same even if one takes into account the valence band anisotropy. The obtained results can be interesting for the design of Si-compatible device structures containing GaN nanocrystals for optoelectronic and photonic applications. We predict that GaN quantum dots should be light-emitting in the UV spectral range. Moreover, their optical gaps rather slightly depend on the properties of surrounding matrix especially for the crystallites of larger sizes (with radii more than 2 nm). This prediction allows one to choose the dielectric matrix that provides the optical technological solution without any significant affect onto the electronic properties of the fabricated system.

The luminescence spectroscopy can be used as an effective tool to understand whether electrons and holes in nanocrystals have the properties of the particles confined in quantum dots. Such quantities like size-dependent "blue shift" of the luminescence spectrum of dielectric film containing nanocrystals are fingerprints that allow one to reveal importance of quantum confinement effect in the system.[9] But the luminescence peak can be broaden into wide spectrum line for ensemble of nanocrystals prepared using ion implantation.[21] As a result the fine structure of the nanocrystal electronic spectrum becomes unresolved in the experiment and it becomes more important to understand just the spectral range where one can find the emission produced by confined carriers. This spectral range is calculated in the work.

ACKNOWLEDGEMENTS

The study is supported by the Ministry of Education and Science of the Russian Federation (Project identifier RFMEFI58414X0008) and the Department of Science and Technology, India (Project No. INT/RUS/RMES/P-04/2014).

The authors would like to thank V.A. Burdov for fruitful discussions.

[1] R. Quay, *Gallium Nitride Electronics* (Springer, 2008).
[2] B. Jayant Baliga, Semiconductor Science and Technology **28**, 074011 (2013).
[3] T. Takeuchi, H. Amano, K. Hiramatu, N. Sawaki, and I. Akasaki, J. Cryst. Growth **115**, 634 (1991).
[4] M. Kumar, B. Roul, T.N. Bhat, M.K. Rajpalke, P. Misra, L.M. Kukreja, N. Sinha, A.T. Kalghatgi, and S.B. Krupanidhi, Materials Research Bulletin **45**, 1581 (2010).

[5] F. Komarov, L. Vlasukova, W. Wesch, A. Kamarou, O. Milchanin, S. Grechnyi, A. Mudryi, and A. Ivaniukovich, Nuclear Instruments and Methods in Physics Research B **266**, 3557 (2008).
[6] E. Wendler, K. Filintoglou, P. Kutza, Ph. Lorenz, K. Lorenz, F.F. Komarov, S. Ves, E. Paloura, and M. Katsikini, in *Abstracts of 19th International Conference on Ion Beam Modification of Materials (IBMM 2014)*, *Leuven, Belgium*, *September 14-19* (2014), B98.
[7] D.S. Korolev, A.N. Mikhaylov, A.I. Belov, V.K. Vasiliev, D.V. Guseinov, E.V. Okulich, A.A. Shemukhin, S.I. Surodin, D.E. Nikolitchev, A.V. Nezhdanov, A.V. Pirogov, D.A. Pavlov, and D.I. Tetelbaum, Semiconductors **50**, 271 (2016).
[8] V.A. Sergeev, D.S. Korolev, A.N. Mikhaylov, A.I. Belov, V.K. Vasiliev, A.E. Smirnov, D.E. Nikolitchev, S.I. Surodin, D.V. Guseinov, A.V. Nezhdanov, A.S. Markelov, V.N. Trushin, A.V. Pirogov, D.A. Pavlov, and D.I. Tetelbaum, Journal of Physics: Conference Series **643**, 012082 (2015).
[9] V.A. Belyakov, V.A. Burdov, R. Lockwood, and A. Meldrum, Advances in Optical Technologies **2008**, 279502 (2008).
[10] O.B. Gusev, A.N. Poddubny, A.A. Prokofiev, and I.N. Yassievich, Semiconductors **47**, 183 (2013).
[11] B. Delley and E.F. Steigmeier, Phys. Rev. B **47**, 1397 (1993).
[12] C. Delerue, M. Lannoo, and G. Allan, Phys. Rev. Lett. **84**, 2457 (2000).
[13] A. Franceschetti and A. Zunger, Phys. Rev. B **62**, 2614 (2000).
[14] A.N. Poddubny, A.A. Prokofiev, and I.N. Yassievich, Appl. Phys. Lett. **97**, 231116 (2010).
[15] J.M. Luttinger and W. Kohn, Phys. Rev. **97**, 869 (1955).
[16] V.A. Burdov, Semiconductors **36**, 1154 (2002).
[17] A.N. Mikhaylov, A.I. Belov, A.B. Kostyuk, I.Yu. Zhavoronkov, D.S. Korolev, A.V. Nezhdanov, A.V. Ershov, D.V. Guseinov, T.A. Gracheva, N.D. Malygin, E.S. Demidov, and D.I. Tetelbaum, Physics of the Solid State **54**, 368 (2012).
[18] E. Borsella, M. A. Garcia, G. Mattei, C. Maurizio, P. Mazzoldi, E. Cattaruzza, F. Gonella, G. Battaglin, A. Quaranta, and F. D'Acapito, J. Appl. Phys. **90**, 4467 (2001).
[19] E. Borsella, C. de Julian Fernandez, M.A. Garcia, G. Mattei, C. Maurizio, P. Mazzoldi, S. Padovani, C. Sada, G. Battaglin, E. Cattaruzza, F. Gonella, A. Quaranta, F. D'Acapito, M.A. Tagliente, and L. Tapfer, Nucl. Instr. Meth. B. **191**, 447 (2002).
[20] E.E. Takhtamirov and V.A. Volkov, JETP **89**, 1000 (1999).
[21] R. Elliman, in *Silicon Nanocrystals: Fundamentals, Synthesis and Applications*, edited by L. Pavesi and R. Turan (Wiley-VCH, 2010), p. 223.
[22] V.V. Batygin and I.N. Toptygin, *Problems in Electrodynamics*, 2nd ed. (Academic Press Inc. (London), Pion Limited, London, 1978).
[23] A. A. Konakov and V. A. Burdov, J. Phys.: Condens. Matter **22**, 215301 (2010).
[24] P. Rebentrost, M. Stopa, and A. Aspuru-Guzik, Nano Lett. **10**, 2849 (2010).
[25] T. Hanada, *Oxide and Nitride Semiconductors. Processing, Properties, and Applications* (Springer, 2009), p. 1.
[26] V. Bougrov, M.E. Levinshtein, S.L. Rumyantsev, and A. Zubrilov, "Gallium nitride (GaN)," in *Properties of Advanced Semiconductor Materials GaN, AlN, InN, BN, SiC, SiGe*, edited by M.E. Levinshtein, S.L. Rumyantsev, and M.S. Shur (John Wiley & Sons, Inc., New York, 2001), pp. 1-30 ISBN: 978-0-471-35827-5.
[27] D.I. Tetelbaum, A.N. Mikhaylov, A.I. Belov, A.V. Ershov, E.A. Pitirimova, S.M. Plankina, V.N. Smirnov, A.I. Kovalev, R. Turan, S. Yerci, T.G. Finstad, and S. Foss, Phys. Solid State **51**, 385 (2009).
[28] J. Robertson and B. Falabretti, J. Appl. Phys. **100**, 014100 (2006).
[29] P. Rinke, M. Winkelnkemper, A. Qteish, D. Bimberg, J. Neugebauer, and M. Scheffler, Phys. Rev. B. **77**, 075202 (2008).
[30] I. Vurgaftman and J.R. Meyer, J. Appl. Phys. **94**, 3675 (2003).
[31] M. Cardona and N.E. Christensen, Solid State Communications **116**, 421 (2000).
[32] V.A. Burdov, JETP **121**, 480 (2002).
[33] Y.N. Fernández, M.I. Vasilevskiy, E.M. Larramendi, and C. Trallero-Giner, in *Fingerprints in the Optical and Transport Properties of Quantum Dots*, edited by A. Al-Ahmadi (INTECH, 2012), p. 199.
[34] L.D. Landau and E. M. Lifshitz, *Quantum Mechanics: Non-Relativistic Theory*, Course of Theoretical Physics Vol. 3 (Nauka, Moscow, 1989, 4th ed.; Pergamon, New York, 1977, 3rd ed.).
[35] M. Suzuki, A. Uenoyama, and T. Yanase, Phys. Rev. B **52**, 8132 (1995).
[36] Al.L. Efros, M. Rosen, M. Kuno, M. Nirmal, D.J. Norris, and M. Bawendi, Phys. Rev. B **54**, 4843 (1996).